

Suppression of photorefraction in hafnium doped lithium niobate crystals

R. K. HOVSEPYAN, A. R. POGHOSYAN*, E. S. VARDANYAN
Institute for Physical Research, Ashtarak-2, 378410, Armenia

Lithium niobate crystals used in quantum electronics and integrated optics are mainly doped by different impurities in order to strengthen or suppress one or another property. Here we discuss the influence of hafnium impurity on photorefractive and photoelectric properties of lithium niobate crystals. The investigations of photorefractive effect in hafnium doped lithium niobate crystals have shown the possibility of suppression of photorefraction in these crystals (up to 3 orders). The experimental results demonstrate that the suppression of photorefraction occurs as a result of correlated increase of crystal dark and photo conductivities by 5 orders which is explained by significant increase of polaron mobility in the conduction band. One of the possible causes of the polaron mobility increase is the modification of the phonon spectrum of the crystal and a reduction of polaron scattering on defects associated with the lithium deficiency.

(Received November 14, 2006; accepted April 12, 2007)

Keywords: Nonlinear optic materials, Photorefraction suppression, Lithium niobate

1. Introduction

Lithium niobate crystals (LiNbO_3) are extensively used in quantum electronics and integrated optics. To use in technical applications these crystals are mainly doped by different impurities in order to intensify or suppress one or another property. The photorefractive effect in lithium niobate crystal restricted its application, but recent achievements in photorefraction suppression have allowed to expand use of lithium niobate crystals in nonlinear optical applications (frequency doubling, modulator and etc.). The possibility of suppression of photorefraction in LiNbO_3 with hafnium impurity was discussed for the first time in the works [1, 2]. In spite of a great number of works concerning the photorefraction suppression in lithium niobate crystals [3-6] there are many interesting problems related to the mechanism of suppression because the mechanisms may be different for different impurities (for example, for Mg, Zn or Hf impurities).

2. Experimental procedures and results

Lithium niobate single crystals were grown by Czochralski method using a charge synthesized from niobium pentoxide and lithium carbonate. Hafnium and iron impurities were added into the melt as relevant oxides. Crystals were grown from the congruent melt ($\text{Li/Nb}=0.946$) nominally pure (overall concentration of uncontrollable impurities was less than 0.001%), doped with Hf (concentration HfO_2 in the melt: 0.016, 0.16, 1.65, 4.0 and 6.0 mol.%), Hf:Fe (0.016:0.027, 0.16:0.027, 1.65:0.027 mol.%) and from stoichiometric melt ($\text{Li/Nb}=1.0$) doped with HfO_2 (0.017, 0.17 and 1.7 mol.%).

Crystal conductivities were measured by an electrometric amplifier (with the impedance $10^{12}\Omega$, 1 pF) using external voltage source (electric field values 100–2000 V/cm). Photoconductivity was measured in the range of the light intensity from 10 mW/cm^2 to 100 W/cm^2 . As the light source we used an argon-ion laser ($\lambda=488$ nm). Experimental results of measurements of dark and

photoconductivities are presented in the Table 2 (columns 5, 6). The dependence of photoconductivity current on the light intensity for the crystal with 6 mol.% of hafnium is shown in Fig. 1. The dependence on light intensity is linear up to 1 W/cm^2 .

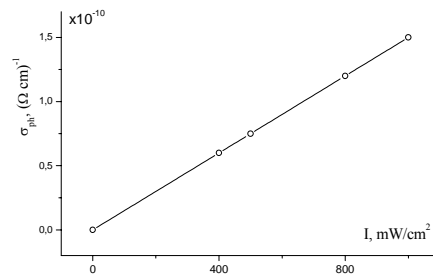


Fig. 1. Dependence of photoconductivity current on light intensity in $\text{LiNbO}_3:\text{Hf}$ (6 at.%) crystal.

The magnitude of the pyroelectric current was measured by means of a synchronous detector and modulated (20 Hz) laser radiation ($\lambda=488$ nm). We used two measurement methods. In the first case laser radiation passed through the crystal and the pyroelectric signal caused by optical absorption was measured. In the second case the crystal face was covered with a light absorbing material so the pyroelectric current was caused by laser power which was fully absorbed at the crystal face. The ratio of magnitudes of these signals allows to determine correctly the absorption coefficient α of the crystal. From the value of the pyrocurrent the pyroelectric constant ($\gamma=dP_s/dT$) was defined for crystals with different impurities. It was found that this constant was practically independent from the impurity. The photovoltaic current was measured by "current-voltage" converter under argon-ion laser radiation ($\lambda=488$ nm). The electrodes were deposited on the crystal Z faces. The value of the bulk photovoltaic current (J_{ph}) is proportional to the light intensity I ($J_{ph} = k\alpha I$, where k is photovoltaic or Glass constant).

The measurements showed that the values of the photovoltaic constant for nominally pure crystals and for crystals doped with Fe (0.027 mol.%) don't differ essentially despite of a large difference in photorefractive sensitivities. This means that photovoltaic centres in nominally pure and iron-doped crystals are same type. At the same time k in lithium niobate crystals doped by Hf or Hf:Fe is three times smaller than in nominally pure crystals (see Table 1). The obtained result (decrease of k constant) may be explained in the frame of the lithium niobate defect structure model proposed in refs. [7-9].

Table 1. Photovoltaic constant k in doped crystals.

| LiNbO ₃ | | k , A cmW ⁻¹ |
|--------------------|------------|------------------------------|
| Hf, mol. % | Fe, mol. % | |
| - | - | 3×10^{-9} |
| 1.65 | - | 2×10^{-9} |
| 4.0 | - | 1×10^{-9} |
| 6.0 | - | 1×10^{-9} |
| - | 0.027 | 3×10^{-9} |
| 0.16 | 0.027 | 2×10^{-9} |
| 1.65 | 0.027 | 1×10^{-9} |

According to this model niobium ions have two positions: its own crystallographic position (Nb_{Nb}) and the position of crystallographic lithium (Nb_{Li}). In a position of crystallographic lithium there is also an uncontrollable iron impurity (Fe²⁺_{Li}). When the stoichiometry is varied from 0.946 to 1.0 the quantity of Nb_{Li} and Fe²⁺_{Li} is decreased. It is known that Li-ions or the ions occupying its positions have the most asymmetric potential well. Therefore Nb_{Li} and Fe²⁺_{Li} ions have more asymmetric potential well than Nb_{Nb} or Fe_{Nb}. As a result photoelectrons exiting from Nb_{Li} or Fe²⁺_{Li} have higher

photovoltaic momentum along the crystal spontaneous polarization than photoelectrons exiting from Nb_{Nb}. Substitution of Fe²⁺_{Li} ions by Hf_{Li} leads also to decrease of k since the light-stimulated transition (Hf⁴⁺ + $h\nu$ → Hf⁵⁺ + e) is impossible due to absence of Hf⁵⁺. The decrease of k in nominally pure near stoichiometric crystals where quantity of Nb_{Li} or Fe_{Li} is minimal shows also in favour of this model. So at Hf concentration exceeding Fe concentration a modification of the photovoltaic centre type occurs and value of k is also changed. But it is necessary to note that decrease of k cannot be a reason of substantial suppression of photorefraction in LiNbO₃ crystals.

The photorefractive sensitivity was measured by three methods. In the first method, an Ar-ion laser radiation transmits through the crystal and the photoinduced change of refractive index n_e is checked. The crystal is considered as stable to laser radiation if the value of induced change of refractive index is lower than 10^{-6} ($\Delta n_e < 10^{-6}$). These data are presented in column 1 of the Table 2. In the second (polarization optical) method the crystal is placed between crossed polarizers and we measure the light induced birefringence $\delta\Delta n$ ($\delta\Delta n \approx \Delta n_e$). We used the light beam ($I=10$ W/cm²) about 1mm diameter corresponding to spatial frequency 10 lines/cm (see column 2, Table 2). In the third, holographic, method, the phase hologram of two plane waves is recorded with spatial frequency 1000 lines/cm. The value Δn_e is determined from the hologram diffraction efficiency according to the Kogelnik theory of coupled waves [10]. The sensitivity (see Table 2, column 3) is determined from the expression $S = \Delta n_e / (I \Delta t)$, when $t \rightarrow 0$.

The relaxation time τ (see Table 2, column 4) is determined from the experimental dependence of the induced birefringence relaxation approximated by a formula $\Delta n_e(t) = \Delta n_e \exp(-t/\tau)$.

Table 2. Photorefractive parameters of lithium niobate crystals.

| LiNbO ₃ | | | Sensitivity | | | τ 4 | σ_{dark} 5 (Ωcm) ⁻¹ | σ_{photo} 6 $\Omega^{-1}\text{W}^{-1}\text{cm}$ |
|--------------------|------------|-------------------|---|---|---|-------------|--|---|
| Hf, mol. % | Fe, mol. % | η (Li/Nb) | 1 I, W/cm ² ($\Delta n < 10^{-6}$) | 2 $\Delta n/I\Delta t$, cm ² /Ws (10 cm^{-1}) | 3 $\Delta n/I\Delta t$, cm ² /Ws (1000 cm^{-1}) | | | |
| - | - | 0.946 | 0.01 | 10^{-8} | 10^{-8} | 1 year | $< 10^{-15}$ | 1×10^{-16} |
| 0.016 | - | 0.946 | 0.01 | 10^{-8} | 10^{-8} | 6 hour | $< 10^{-15}$ | 0.8×10^{-14} |
| 0.032 | - | 0.946 | 0.01 | 10^{-9} | 10^{-8} | 6 hour | 1×10^{-14} | 0.8×10^{-14} |
| 0.16 | - | 0.946 | 0.1 | 10^{-9} | 10^{-8} | 1 hour | 6×10^{-14} | 0.4×10^{-12} |
| 1.65 | - | 0.946 | 1 | 10^{-9} | 10^{-8} | 1 hour | 6×10^{-14} | 0.4×10^{-12} |
| 4 | - | 0.946 | 10 | 10^{-11} | 10^{-8} | 10 min | 4×10^{-13} | 0.1×10^{-12} |
| 6 | - | 0.946 | 100 | 10^{-13} | 10^{-10} | 5 sec | 5×10^{-10} | 1.5×10^{-10} |
| - | 0.027 | 0.946 | 10^{-4} | 10^{-5} | 10^{-5} | 1 year | $< 10^{-15}$ | $< 10^{-16}$ |
| 0.016 | 0.027 | 0.946 | 10^{-4} | 10^{-5} | 10^{-5} | 6 hour | $< 10^{-15}$ | $< 10^{-16}$ |
| 0.16 | 0.027 | 0.946 | 10^{-3} | 10^{-6} | 10^{-5} | 6 hour | 4×10^{-14} | 0.4×10^{-12} |
| 1.65 | 0.02 | 0.946 | 10^{-3} | 10^{-7} | 10^{-5} | 10 min | 4×10^{-13} | 0.4×10^{-12} |
| 0.016 | - | 0.98 | 0.01 | 10^{-8} | 10^{-8} | 6 hour | 1×10^{-14} | 0.9×10^{-12} |
| 0.16 | - | 0.98 | 1 | 10^{-10} | 10^{-8} | 6 hour | 1×10^{-14} | 0.8×10^{-12} |
| 1.65 | - | 0.98 | 10 | 10^{-11} | 10^{-8} | 10 min | 4×10^{-13} | 1.5×10^{-10} |

Raman scattering spectra were measured by DFS-24 spectrometer (spectral width $< 0.5 \text{ cm}^{-1}$) at excitation by a He-Ne laser ($\lambda=632 \text{ nm}$, power 10 mW). The recording system is operated in the photon counting regime with computer processing. All measurements were performed at room temperature. Fig. 2 shows RS-spectra of $\text{LiNbO}_3:\text{Fe}$ and $\text{LiNbO}_3:\text{Fe}:\text{Hf}$ crystals in the scattering geometry X(ZX)Y (a) and X(ZZ)Y (b). Geometry is described in notations used in [11]. Experiments showed that with an increase of Hf concentration a frequency of E(TO) line (152 cm^{-1}) is shifted (up to 155 cm^{-1}) and, additionally, the amplitude of line is decreased and the linewidth is increased. Along with raising of the impurity concentration we observed broadening and merging fundamental modes $A_1(\text{TO})$ ($254\text{-}274 \text{ cm}^{-1}$) into a one broad band. These fundamental modes correspond to active phonons in the range of fundamental frequencies which are caused by the motion of Nb ions (inside the NbO_6 octahedron) along the polar axis [12]. No change in frequencies or other parameters of the other fundamental lines were observed.

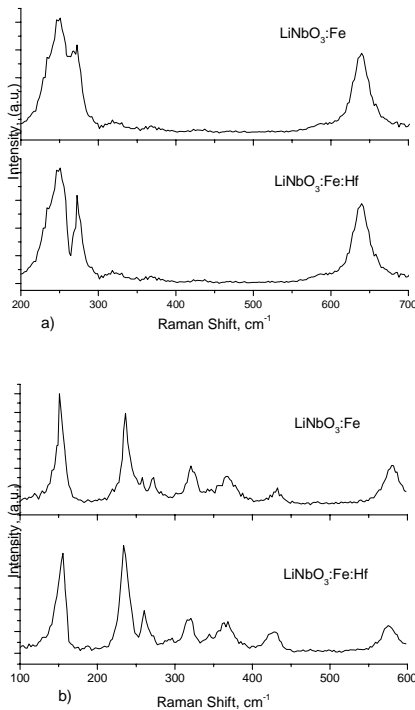


Fig. 2. Raman spectra of lithium niobate crystals: a) vibration modes $A_1(\text{TO})$, scattering geometry X(ZX)Y; b) – vibration modes E(TO), scattering geometry X(ZZ)Y.

3. Discussion

Following well-known photorefractive mechanisms we can write total electric current leading to charge separation as [12]

$$J = (\sigma_d + \sigma_{ph}) E(z,t) + eD \frac{\partial n(z,t)}{\partial z} + k\alpha I \quad (1)$$

The first component describes charge carrier current in induced electric field $E(z,t)$ determining photorefractive via electrooptic effect ($\Delta n_e = -0.5 n_e^3 r_{eff} E$). Here σ_d and σ_{ph} are dark and photoconductivity respectively, r_{eff} – effective electrooptic coefficient. The second component describes the diffusion current of photoelectrons in the conduction band, where D is diffusion coefficient, $n(z,t)$ – electron concentration in the conduction band, z – spatial coordinate along Z axis. The third component describes the photovoltaic current (k is photovoltaic constant, α – absorption coefficient, I – light intensity). The differential equation (1) can be analytically solved in two extreme cases: $t=0$ and $t=\infty$. It is obvious that $J=0$ when $t=\infty$, i.e. photovoltaic and diffusive currents are compensated by an opposite current. In this case the photoinduced electric field is $E(z,\infty) = E_{ph}(z,\infty) + E_d(z,\infty)$, where $E_{ph}(z,\infty)$ is the field caused by photovoltaic current and $E_d(z,\infty)$ is the field caused by diffusion mechanism of charge separation:

$$E_{ph}(z,\infty) = \frac{k\alpha I}{\sigma_d + \sigma_{ph}}, \quad (2)$$

$$E_d(z,\infty) = \frac{eD \frac{\partial n(z)}{\partial z}}{\sigma_d + \sigma_{ph}}$$

According to equation (2), E_{ph} depends linearly on k , therefore reduction of k (see Table 1) can not be the reason of the photorefractive suppression in Hf doped crystals.

The carrier concentration in the conduction band at the recording of holographic grating may be described by the expression $n(z) = \alpha I [(1 + \sin(Kz))]$, where K is the spatial frequency vector of the interference pattern. Taking into account an expression $D = k_B T \mu^* / e$, where μ^* is photoelectron mobility in the conduction band, we obtain the equation for diffusion electric field:

$$E_d(z,\infty) = \frac{k_B T \mu^* K n_{ph}}{e(n_d \mu_d^* + n_{ph} \mu_{ph}^*)} \quad (3)$$

Note that in the first and second methods of photorefractive measurement $E_d \approx 0$ because in these methods $K \approx 0$. If photon energy does not greatly exceed the forbidden band energy and, as a result, the thermalization time for photoexcited electrons is much shorter than the lifetime of these carriers in the conduction band, then we can consider $\mu_d^* = \mu_{ph}^*$. Thermalization time is the time during which the photoexcited electron loses its energy and relaxes to the bottom of conductivity band. From eq. (3) we can see that the photorefractive electric field E_d caused by diffusive mechanism does not depend on the mobility of electrons. So it can decrease only due to increase of concentration n_d . But when the photovoltaic mechanism is predominant, we have

$$E_{ph}(z,\infty) = \frac{k\alpha I}{e(n_d \mu_d^* + n_{ph} \mu_{ph}^*)} \quad (4)$$

Apparently, that photorefractive electric field $E_{ph}(z, \infty)$ caused by photovoltaic mechanism depends both on concentration n_d and electron mobility. Taking into account that electrooptic effect is a single mechanism of Δn_e change, we can conclude that when only charge carrier mobility rises the induced change of refractive index caused by diffusion mechanism is not changed, while Δn_e caused by photovoltaic mechanism is decreased.

The photorefraction studies carried out by different methods have allowed to reveal the relative contributions of the various mechanisms and also to find out the mechanism of an influence of Hf impurity. Data presented in col. 1 and 2 show influence of Hf impurity only on photovoltaic component as in this case $E_d=0$ (because of $K=0$). Data shown in column 3 allow to define effect of Hf impurity on holographic (diffusion) component. Obviously that Hf impurity leads to decrease of photovoltaic component, but holographic component is not considerably changed. It means that adding of Hf impurity essentially increases photoelectron mobility, practically not changing charge carrier concentration. The last conclusion is confirmed by our experimental results (see Table 2).

Fig. 3 shows the time dependence of Δn_e in the cases of polarization optical (1) and holographic (2) measurements. The following is observed experimentally: for pure and iron-doped crystals the measured values of Δn_{st} in two methods are comparable, which indicates the predominance of photovoltaic mechanism of charge separation. In $\text{LiNbO}_3:\text{Hf}$ and $\text{LiNbO}_3:\text{Fe}:\text{Hf}$ crystals these values are totally different: the holographic sensitivity is much higher than the polarization optical one. This fact may be explained only by the mobility increase.

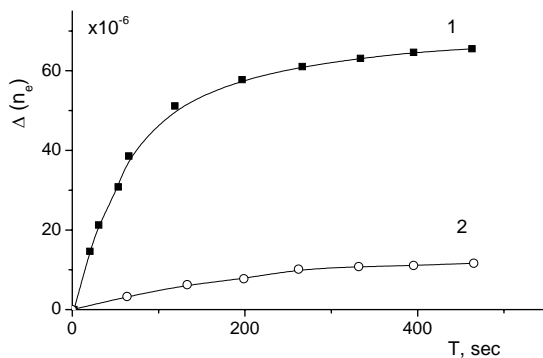


Fig. 3. Time dependence of photoinduced change of refractive index in $\text{LiNbO}_3:\text{Hf}$ (6 mol.%) measured by holographic (1) and polarization optical (2) methods.

Dark and photo- conductivities of the crystals are described by the expressions: $\sigma_d = en_d\mu$ and $\sigma_{ph} = en_{ph}\mu$. Experimental data on the correlated increase of dark and photo conductivities depending on Hf impurity concentration (see columns 5, 6 in Table 2) are also

evidence of mobility increase and, as corollary, increase of conductivity and decrease of a relaxation time.

Consider now the possible mechanisms of charge carrier mobility change. We think such an abrupt change can not be explained by the change of the constant of electron-phonon interaction, since it would cause also a change of the crystal nonlinear susceptibility, which is not experimentally observed. The carrier mobility in the conduction band depends on the scattering mechanism (we assume a single valley parabolic band). In lithium niobate crystals the bond between O^{2-} and Nb^{5+} ions is predominantly covalent and considerably stronger than O^{2-}Li^+ bond, which is purely ionic. So it seems realistic to assume that electrons in the conduction band are dissipated mainly by longitudinal acoustic (LA) phonons. The LA modes cause local modulation of the dielectric constant. In Raman scattering and infrared absorption of lithium niobate crystals there are A_1+E acoustical and $5A_2$ optical inactive vibrations which is not seen in RS and IR spectra. Therefore, the direct registration of LA modes is impossible, but their changes can be indirectly observed in the spectra of the allowed optical modes. Transverse phonons which can scatter conductivity electrons should have a wavelength not shorter than the electron wavelength (polaron size).

Therefore the anomalous conductivity increase caused by Hf impurity may be associated with two phonon mechanisms of mobility increase. In first case Hf impurity leads to reduction of quantity of ionized vacancy defects [13, 14], formed by Nb ions and impurities occupying lithium sites. Thus effectiveness of the polaron scattering is decreased. In second case the intensity of long-wave acoustical phonon modes may be decreased due to creation of Hf sublattice. These modes give main contribution to the polaron scattering and thus define the mobility value.

4. Conclusion

The influence of Hf impurity on photorefractive and photoelectric properties of LiNbO_3 crystals has been studied. The obtained experimental results demonstrate that the suppression of photorefraction in these crystals occurs as a result of correlated increase of dark and photo conductivities (by 5 orders). Measurements show that with the increase of Hf concentration the polarization optical photorefractive sensitivity is reduced while the holographic sensitivity is not practically changed. These experimental results are explained by increase of polaron mobility in the conduction band. One of the possible reasons of the polaron mobility increase is the modification of the phonon spectrum of the crystal and a reduction of polaron (photoelectron) scattering on defects associated with the lithium deficiency.

Acknowledgements

The authors would like to acknowledge the partial financial support for this work by CRDF/NFSAT Award number ARE2-3238-AS-04.

References

- [1] G. T. Avanesyan, E. S. Vardanyan, R. K. Hovsepyan, A. R. Poghosyan, *Phys.Stat.Sol.(a)*, **126**, 245 (1991).
- [2] E. S. Vardanyan, L. M. Kazaryan, R. K. Hovsepyan, A. R. Poghosyan, *Crystallography*, **44**, 1 (1999).
- [3] T. Volk, M. Wohlecke, N. Rubinina, N. V. Razumovski, F. Jermann., C. Fischer, *Appl. Phys. A*, **60**, 217 (1995).
- [4] L. Razzari, P. Minzioni, I. Cristiani, V. Degiorgio, E. P. Kokanyan, *Applied Phys. Letters*, **86**, 131914 (2005).
- [5] I. A. Ghambaryan, R. Guo, R. K. Hovsepyan, A. R. Poghosyan, E. S. Vardanyan, V. G. Lazaryan, *J. Optoelectron. Adv. Mater.* **5**, 61 (2003).
- [6] C. Prieto, C. J. Zaldo, *Phys., Condens. Matter.*, **L6**, 677-682 (1994).
- [7] O. F. Schirmer, S. M. Tomlinson, M. Wohlecke, *J. Phys. Chem. Solids* **52**, 185, (1991).
- [8] H. Donnerberg, S. M. Tomlinson, R. A. Catlow, O. F. Schirmer, *Phys. Rev. B*, **40**, 909 (1989).
- [9] H. Donnerberg, S. M. Tomlinson R. A. Catlow, O. F. Schirmer, *Phys. Rev. B*, **44**, 4877 (1991).
- [10] H. Kogelnik, *Bell Syst. Tech. J.*, **48**, 2909 (1969).
- [11] N. V. Sidorov, M. N. Palatnikov, V. T. Kalinnikov, *J. of Optica and Spectroscopiya*, **82**, 38 (1997).
- [12] M. Lines, A. M. Glass, *Principles and applications of ferroelectrics*, Oxford Univ., Oxford (1971).
- [13] U. Schlarb, S. Klauer, K. Betzler, M. Wohlecke, *Appl. Phys. A*, **56**, 311 (1993).
- [14] C. Prieto, C. Zaldo, H. Dexpert, P. Fossla, *J Phys Condens. Matter.*, **3**, L 4435 (1991).

*Corresponding author: arp@ipr.sci.am